ELSEVIER

Active damping of a beam using a physically collocated accelerometer and piezoelectric patch actuator

Gianluca Gatti[a],*, Michael J. Brennan[b], Paolo Gardonio[b]

[a]*Department of Mechanical Engineering, University of Calabria, Arcavacata di Rende (CS) 87036, Italy*
[b]*Institute of Sound and Vibration Research, University of Southampton, Southampton SO17 1BJ, UK*

Abstract

This paper presents a theoretical and experimental study of the active vibration control of a simply supported beam using a piezoelectric patch actuator and a physically collocated accelerometer. Direct velocity feedback (DVFB) control is used to attenuate unwanted vibrations in a given frequency band. The performance of the control system is presented in terms of the total vibrational kinetic energy of the beam and compared to the fundamental limitation, for the particular actuator, by way of a feedforward control analysis.

Since the sensor and actuator are not collocated in the control sense, the control system is only conditionally stable. The stability is also influenced by the actual control system electronics and the transducer dynamics, which results in even lower stability margins. It is shown in this paper that for a given electronics system and transducer arrangement, improvements can be made by inserting a concentrated mass at the sensor location so as to cause an additional roll-off of the open-loop frequency response function at higher frequencies. This improves the stability margin of the overall control system and hence permits a higher control gain.

© 2007 Elsevier Ltd. All rights reserved.

1. Introduction

The theory of active control of flexible structures is a well-established technique. This may be achieved either by feedforward or feedback control strategies, and a comprehensive review of such systems has been conducted by Alkhatib and Golnaraghi [1]. The feedforward technique [2] is often used whenever a signal correlated to the disturbance is available. In the most ideal case, the disturbance can be completely eliminated at the location of the sensors (local control), but there is no guarantee that the global response is also reduced. Active damping is usually achieved using feedback controllers [3,4] and aims to reduce the vibration at frequencies close to structural resonances, thus achieving global control.

To the authors' knowledge, the active control of beam vibrations was first introduced by Rockwell and Lawther [5] in 1964, and in 1987 a comprehensive review of this subject was conducted by Mace [6]. The active

---

*Corresponding author. Tel.: +39 (0)984 494939; fax: +39 (0)984 494673.

E-mail address: g.gatti@unical.it (G. Gatti).

damping of beam vibration using smart materials has been subsequently investigated by researchers over the past two decades. In more recent years, several studies have been presented, which discuss and compare different active control approaches, such as positive position feedback (PPF) [7,8], strain rate feedback (SRF) [8,9] and direct velocity feedback (DVFB) [7,10]. PPF control is applied by feeding the structural position directly to a compensator, whose output is fed through a fixed gain positively back to the structure, thus achieving damping for a particular mode. In SRF, the derivative of the voltage from a piezoelectric patch sensor (which is proportional to the strain rate) is fed to the input of a compensator, which applies its negative output voltage to an actuator. SRF has a wider active damping region, as compared to PPF, and can stabilise more than one mode. DVFB could be considered as the simplest way to implement active damping, since the velocity signal measured by a sensor is electronically multiplied by a fixed gain and fed directly back to an actuator.

Conventional collocated point sensor and actuator pairs offer an extremely effective way to implement robust active feedback control systems, particularly when DVFB is used [11,12]. This strategy is unconditionally stable for any type of primary disturbance acting on a structure, despite having a very simple controller. In practice, non-collocated sensor and actuator pairs are often used due to physical limitations of the system. This will affect the closed-loop system stability [13,14]. Among sensors and actuators, piezoceramic elements have been used to suppress unwanted structural vibrations since 1987 [15]. Feedback control has been used with a non-collocated velocity sensor and a moment-pair generated by a piezoceramic element by Burdess and Fawcett [16] and in the work by Variyart et al. [17]. Other aspects of this actuator–sensor pair in a feedback control system have been studied previously by Hong and Elliott [18] and Gardonio and Elliott [19].

In the present work, DVFB control of a flexible beam is further investigated, using a physically collocated accelerometer and a piezoelectric patch actuator applied to the structure. The aim of this paper is to explore the limits of DVFB control, which is possibly the simplest feedback control strategy, and to compare the results with the best that could be achieved with the same actuator and sensor configuration, i.e. feedforward control. The control problem is formulated up to about 3 kHz as a vibro-acoustic problem, where the mean vibration reduction over a low audio frequency range is desired. The performance of the control system is presented in terms of the total vibrational kinetic energy of the beam. Simulations are presented along with some experimental results.

Throughout the paper a damping ratio of 0.01 is assumed for the beam. The improvement in the performance of the DVFB control system achieved by attaching a point mass to the beam at the sensor location is investigated by way of some simulations.

2. Fundamental limitation of active vibration control

There is a fundamental limit to the performance of an active vibration control system for a given actuator and sensor configuration in terms of the kinetic energy of the structure. This can be determined by conducting an analysis of the feedforward control of the system.

Consider the aluminium beam depicted in Figs. 1a and b with two PZT actuator patches attached to it, one of which acts as the primary excitation source and the other as the secondary source. The dimensions and the material properties of the beam and actuators are given in Tables 1 and 2, respectively. It is assumed that the beam in Fig. 1 has simple supports and Euler–Bernoulli beam theory is used. This theory only approximates the dynamic behaviour of the beam at higher frequencies, but is sufficient for the purposes of this paper. Assuming harmonic vibrations, the time-averaged total vibrational kinetic energy of the structure is given by [2]

$$\mathrm{KE} = \frac{m}{4}\mathbf{q}^{\mathrm{H}}(\omega)\mathbf{q}(\omega), \tag{1}$$

where $\mathbf{q}(\omega)$ is the vector of velocity modal amplitudes and the superscript H denotes the Hermitian transpose, m is the mass of the beam and ω the circular frequency. The relationship between the two moment-pairs that are applied to the beam by the piezoelectric patch actuators, M_p and M_s, is given by $M_s = G(j\omega)M_p$, where
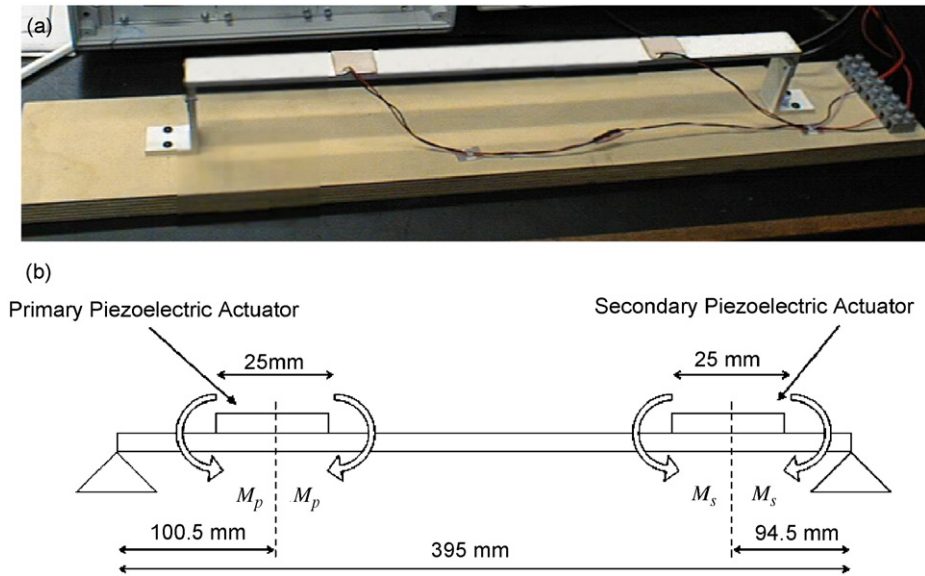
Fig. 1. Beam with attached piezoelectric actuators: (a) picture, (b) sketch.

Table 1
Beam properties

Length (mm)	Width (mm)	Thickness (mm)	Young's modulus (N m^{-2})	Mass density (kg m^{-3})
395	25	5	7.1e10	2700

Table 2
Piezoelectric actuator properties

Length (mm)	Width (mm)	Thickness (mm)	Young's modulus (N m^{-2})	Dielectric constant (m V^{-1})
25	25	1	6e10	212e−12

$G(j\omega)$ is the frequency response of the feedforward controller [2]. The vector of velocity modal amplitudes may be written as

$$\mathbf{q}(\omega) = \mathbf{q_p}(\omega) + \mathbf{q_s}(\omega)G(j\omega), \qquad (2)$$

where $\mathbf{q_p^T}(\omega) = \{q_{p1}(\omega), q_{p2}(\omega), \ldots, q_{pn}(\omega)\}$ and $\mathbf{q_s^T}(\omega) = \{q_{s1}(\omega), q_{s2}(\omega), \ldots, q_{sn}(\omega)\}$ are the vectors of velocity modal amplitudes due to the primary and secondary sources, respectively, where

$$q_{pn}(\omega) = \frac{M_p\omega\big(\phi'_n\big(x_p - (d_p/2)\big) - \phi'_n\big(x_p + (d_p/2)\big)\big)}{m(\omega_n^2(1 + j\eta) - \omega^2)}$$

and

$$q_{sn}(\omega) = \frac{M_s\omega\big(\phi'_n\big(x_s - (d_s/2)\big) - \phi'_n\big(x_s - (d_s/2)\big)\big)}{m(\omega_n^2(1 + j\eta) - \omega^2)}$$

with ϕ'_n denoting the spatial derivative of the nth mode shape, x_p and x_s denoting the coordinates of the central positions of the actuators, respectively, η denoting the loss factor of the beam, and d_p and d_s are the

lengths of the primary and secondary actuators, respectively. Substituting Eq. (2) into Eq. (1) gives

$$\text{KE} = \frac{m}{4}[G^*\mathbf{q_s^H q_s}G + G^*\mathbf{q_s^H q_p} + \mathbf{q_p^H q_s}G + \mathbf{q_p^H q_p}],\qquad(3)$$

where the superscript * denotes the complex conjugate and the dependence on frequency has been omitted for clarity, as will be done henceforth in the paper. This has a global minimum [2] when $G = -[\mathbf{q_s^H q_s}]^{-1}\mathbf{q_s^H q_p}$, which is given by

$$\text{KE}_{\min} = \frac{m}{4}\mathbf{q_p^H}[\mathbf{I} - \mathbf{q_s}[\mathbf{q_s^H q_s}]^{-1}\mathbf{q_s^H}]\mathbf{q_p}.\qquad(4)$$

The minimum kinetic energy that can be achieved using the single primary and secondary piezoelectric actuators can be calculated using Eq. (4), and this is plotted, together with the kinetic energy without control in Fig. 2a for a unit primary moment-pair applied.

To compare the theoretical predictions with measurements, it is necessary to know the relationship between the applied voltage, V, to the piezoelectric actuator, and the moment-pair, M, applied to the beam. This is given by [20]

$$\frac{M}{V} = d_{31}\left(\frac{6E_b I_b}{t_b t_p}\right)\left(\frac{\hat{E}\hat{T}(1+\hat{T})}{1 + 4\hat{T}\hat{E} + 6\hat{T}^2\hat{E} + 4\hat{T}^3\hat{E} + \hat{T}^4\hat{E}^2}\right),$$

where d_{31} is the dielectric coefficient of the piezoelectric actuator given in Table 2, E_b is the Young's modulus of the beam, t_b and t_p are the thicknesses of the beam and piezoelectric actuator, respectively, and $\hat{T} = t_p/t_b$, $\hat{E} = E_p/E_b$, where E_p is the Young's modulus of the piezoelectric actuator.

The kinetic energy of the beam may also be calculated from measured data. This is achieved by measuring the velocity at an equidistant number of points on the beam and using the relationship

$$\frac{\text{KE}}{|M_p|^2} \approx \frac{m}{4r}\mathbf{y^H y},\qquad(5)$$

where $\mathbf{y^T} = \{Y(x_1), Y(x_2),\ldots,Y(x_r)\}$ is the r-length vector representing the velocities per unit primary excitation at r positions on the beam. This can be written in terms of the mobility vectors $\mathbf{y_p}, \mathbf{y_s}$ so that

$$\mathbf{y}(\omega) = \mathbf{y_p} + \mathbf{y_s}G,\qquad(6)$$

where $\mathbf{y_p^T} = \{Y_{p1}, Y_{p2},\ldots,Y_{pr}\}$ and $\mathbf{y_s^T} = \{Y_{s1}, Y_{s2},\ldots,Y_{sr}\}$, with the mobilities given by

$$Y_{pr} = \frac{v(x_r)}{M_p} = j\omega\sum_{n=1}^{\infty}\frac{\phi_n(x_r)}{M_n(\omega_n^2(1+j\eta) - \omega^2)}\left(\phi_n'\left(x_p - \frac{d_p}{2}\right) - \phi_n'\left(x_p + \frac{d_p}{2}\right)\right)$$

and

$$Y_{sr} = \frac{v(x_r)}{M_s} = j\omega\sum_{n=1}^{\infty}\frac{\phi_n(x_r)}{M_n(\omega_n^2(1+j\eta) - \omega^2)}\left(\phi_n'\left(x_s - \frac{d_s}{2}\right) - \phi_n'\left(x_s + \frac{d_s}{2}\right)\right),$$

respectively, where $v(x_r)$ is the lateral velocity of the beam at the rth position. Substituting Eq. (6) into Eq. (5) and following the procedure given in Ref. [2] the gain that minimises the kinetic energy can be determined. It is given by $G = -[\mathbf{y_s^H y_s}]^{-1}\mathbf{y_s^H y_p}$ and the resulting kinetic energy by

$$\frac{\text{KE}_{\min}}{|M_p|^2} = \frac{m}{4r}\mathbf{y_p^H}[\mathbf{I} - \mathbf{y_s}[\mathbf{y_s^H y_s}]^{-1}\mathbf{y_s^H}]\mathbf{y_p}.\qquad(7)$$

An experiment was conducted to measure the kinetic energy of the beam. It was excited by each piezoelectric actuator in turn and the corresponding velocities at 13 equidistant points were measured on the beam using a Polytec's PSV-300 scanning laser vibrometer.

The kinetic energy of the beam was calculated using experimental data. Using the formulation described above the kinetic energy without control and that predicted if feedforward control was applied, is calculated
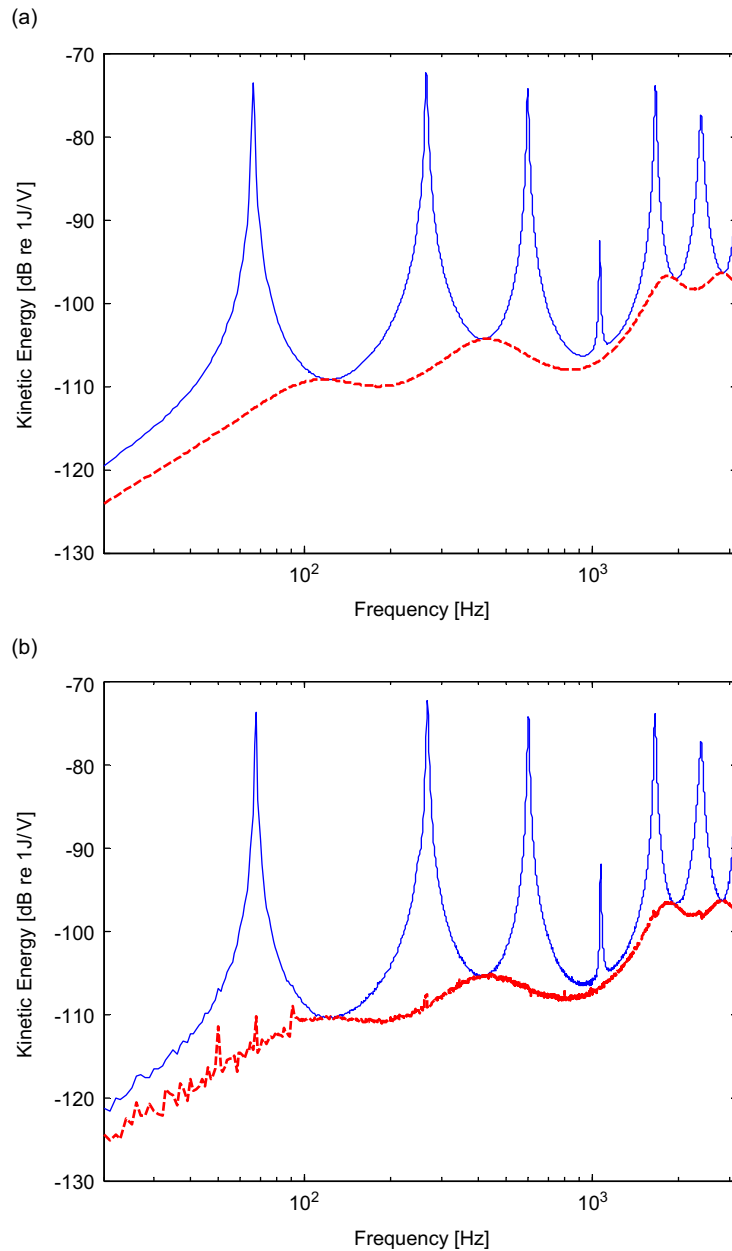
(a)

(b)

Fig. 2. Kinetic energy of the simply supported beam with and without feedforward control: —— uncontrolled; - - - - optimally controlled: (a) theoretical simulation, (b) simulation based on measured data.

and plotted in Fig. 2b. Comparing Figs. 2a and b, it can be seen that there is good agreement between the theoretical and the measured results, which validates the assumption about the boundary conditions and damping in the beam.

One way of quantifying the control performance as a single number is to calculate the area under the graph of the kinetic energy as a function of frequency with and without control, and then forming their ratio to give the overall kinetic energy reduction in the frequency band of interest (0–3.2 kHz) [11]. The theoretical and experimental results are calculated to be −11.46 and −11.51 dB, respectively.
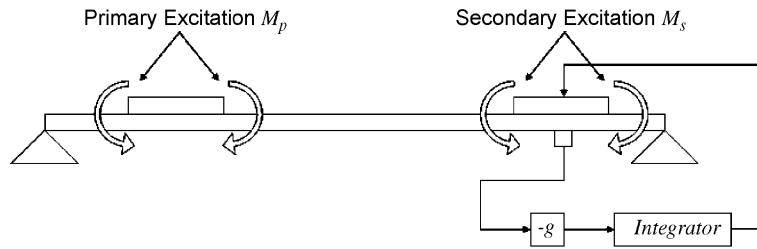
Fig. 3. Velocity feedback control system.

3. Direct velocity feedback control

In this section, some experiments using velocity feedback control are described, and the results are compared with those in the previous section. For the feedforward control strategy discussed above, the optimisation was conducted at each frequency, but in feedback control all frequencies are considered at the same time. The aim is to investigate the degradation of performance if access to the primary source is not possible and the simplest possible feedback control system is implemented. Consider the system shown in Fig. 3, in which the feedback system is depicted. An accelerometer is used as the sensor (whose output is integrated to give velocity), and although it is positioned in the centre of the piezoelectric actuator patch it is not collocated in the control sense ('energetically collocated' according to Preumont [3]), since the moments that are applied to the beam are at the ends of the actuator. Thus, the control system will only be conditionally stable [3].

The secondary moment-pair acting on the beam is related to the measured velocity by

$$M_s = -gv_s,$$ (8)

where g is the feedback gain and v_s is the velocity of the beam at the sensor location, which may also be expressed as a combination of the velocity provided by the primary and secondary excitation as

$$v_s = Y_{ps}M_p + Y_{ss}M_s,$$ (9)

where Y_{ps} and Y_{ss} are the mobilities of the beam at the sensor location due to the primary and secondary excitations, respectively. The relationship between the primary and secondary moment-pairs may thus be obtained by substituting Eq. (8) into Eq. (9) and rearranging to give

$$M_s = M_p \frac{-gY_{ps}}{1 + gY_{ss}}.$$ (10)

The kinetic energy can be determined using Eq. (1), where the vector of modal amplitudes is now given by

$$\mathbf{q} = \mathbf{q_p} + \mathbf{q_s} \frac{-gY_{ps}}{1 + gY_{ss}}.$$ (11)

Ignoring stability issues for the moment (they will be addressed later), it is helpful to consider the system depicted in Fig. 3 under two extreme conditions: that of zero gain and infinite gain. The predicted kinetic energy of the beam under these conditions is plotted in Fig. 4. It is evident that the effect of control in this case is not to add damping to the structure, but to change the properties of the structure such that it has new resonance frequencies, as discussed by Gardonio and Elliot [19]. The actuator has created an active boundary condition, whereby, at the position of the accelerometer the lateral displacement of the beam is significantly decreased. At this position, the shear force is also very small and the bending moment is very large. Comparing Fig. 4 with Fig. 2a, it is clear that (fortunately) a smaller gain is required if the response at the original resonance frequencies is to be reduced without amplifying the response at the new resonance frequencies.

The optimum gain can be calculated by plotting the total kinetic energy reduction as a function of the feedback gain as shown in Fig. 5 to give an approximate value of about 10^4 N s. Also plotted in Fig. 5 is the point at which the system becomes unstable. The Nyquist and Bode plots of the predicted open-loop frequency response function (FRF) of the system are depicted in Figs. 6a and b, respectively. It can be seen that the
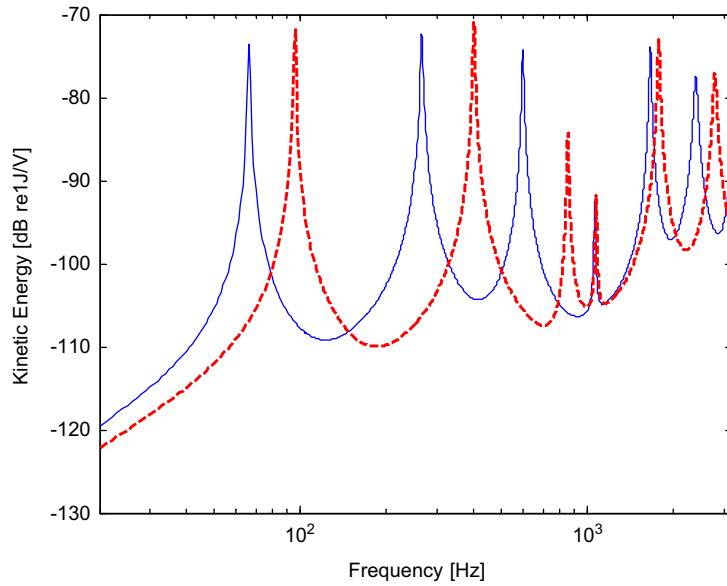
Fig. 4. Kinetic energy of the beam: —— $g = 0$ Ns (uncontrolled); - - - - $g \rightarrow \infty$ N s.
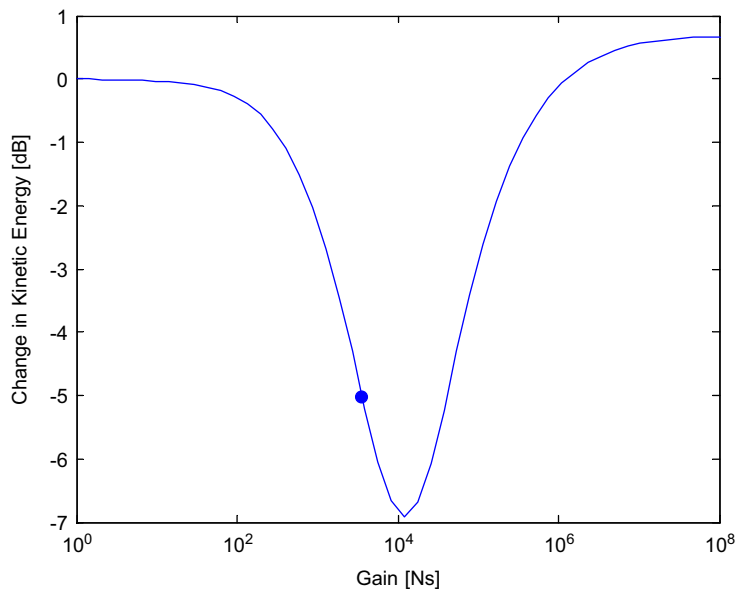

Fig. 5. Change in kinetic energy in the frequency band 0–3.2 kHz using DVFB. The dot denotes the gain at which the system becomes unstable.

frequency at which the system becomes unstable is about 67 kHz, corresponding to a critical gain of about 3600 N s. The wavelength in the beam at this frequency is about 25 mm, which is the length of the actuator. The gain could be increased by shortening the actuator, but then it would be more difficult to excite the beam at lower frequencies as discussed by Brennan et al. [20].

To illustrate the attenuation that could be achieved with this gain, the kinetic energy of the beam with and without control is shown in Fig. 7. By comparing this with Fig. 2a, it can be seen that although there is significant reduction in the kinetic energy at frequencies close to the resonance frequencies, the overall
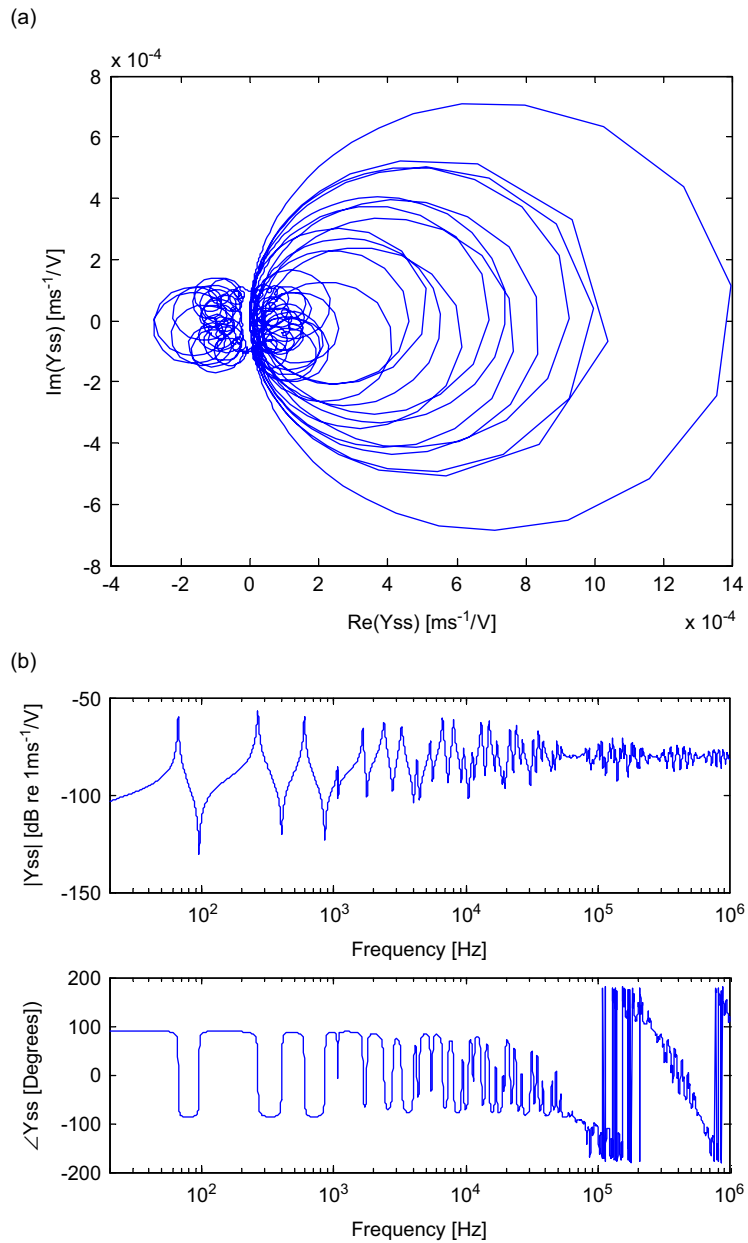
(a)

(b)

Fig. 6. Open-loop FRF (theoretical simulation): (a) Nyquist plot, (b) Bode plot.

performance of the feedback control system is inferior compared with the feedforward control system and the actual reduction that could be achieved could be about 5 dB.

In a real system, the stability and performance are also influenced by the FRFs of the instrumentation as well as the structure to be controlled. In the simple system considered here, this consists of an accelerometer/ signal conditioner (PCB model 352C22/442C04), with FRF H_a, an in-house manufactured integrator/power amplifier unit H_i and the PZT actuator H_p. In this case, the vector of velocity modal amplitudes is given by

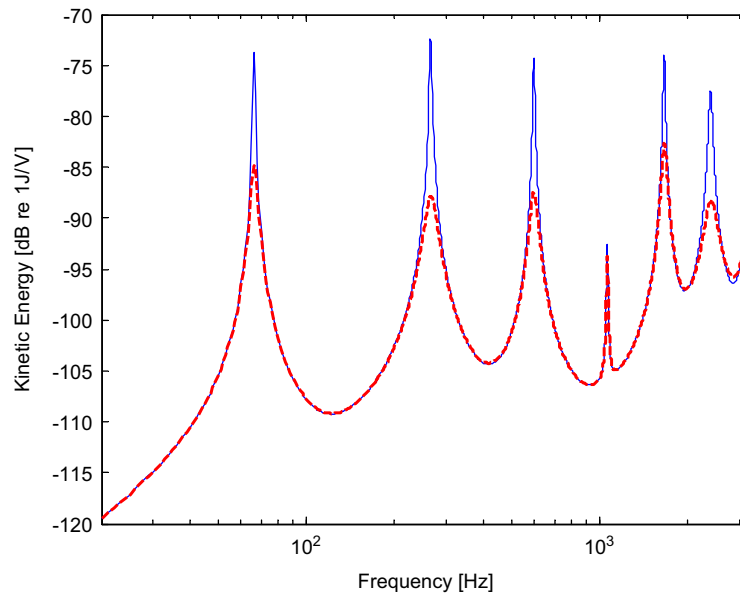$$\mathbf{q} = \mathbf{q_p} + \mathbf{q_s} \frac{-gH_iH_aH_pa_{ps}}{1 + gH_iH_aH_pa_{ss}}, \tag{12}$$

Fig. 7. Kinetic energy of the beam with and without velocity feedback control (theoretical simulation): —— uncontrolled; - - - - $g = 3600 \, \text{N s}$.

where a_{ps} and a_{ss} are the accelerances at the sensor location due to the primary and secondary moment-pair, respectively.

The frequency response of the accelerometer/signal conditioner and the piezoelectric actuator were measured together with that of the beam. This is shown in Fig. 8a and is compared with a theoretical prediction of the accelerance of the beam alone. It can be seen that the measured and predicted results start to deviate above about 10 kHz, and the resonance at about 35 kHz is probably due to the accelerometer. The FRF of the integrator and power amplifier unit is shown in Fig. 8b. It can be seen that the phase begins to deviate from the ideal just below 1 kHz and that the amplitude also starts to deviate above about 10 kHz.

The effects that these components have on the performance of the system can be evaluated by substituting the measured FRFs into Eq. (12) and combining this with Eq. (1). Figs. 9a, b shows the Nyquist and Bode plots of the open-loop FRF of the experimental control system, while the total kinetic energy reduction is shown in Fig. 10 together with that in the ideal case when the instrumentation is assumed to be perfect. The gain at which the system becomes unstable is also marked. It can be seen that the instrumentation is detrimental to both the performance and stability; the integrator and amplifier unit being the main cause of the reduction in performance and only about 3 dB reduction would be possible in a realistic system.

Using the setup shown in Fig. 11, an experiment was conducted in which the feedback system was implemented and different gains were applied. The acceleration signal from the accelerometer was supplied to the signal conditioner and then integrated and amplified by the power unit, which fed the signal back to the secondary piezoelectric actuator. For each gain, the velocities of all the thirteen points were measured according to the experimental procedure described in Section 2 and the total kinetic energy reduction of the system in the frequency range of 0–3.2 kHz was calculated using Eq. (5).

The experimental result is compared to the simulation based on experimental data in Fig. 12. It can be seen that the performance is consistent and slightly less than that predicted in the simulation. It can also be seen that there is a sudden increase in the kinetic energy in the experimental system due to instability.

4. Improving the performance of the velocity feedback control system

The fundamental problem with the combination of a piezoelectric actuator and an accelerometer is that the open-loop frequency response of the beam does not roll-off with frequency, so that the phase-lag in the feedback loop is critically important. One way to overcome this problem would be to use PPF control as
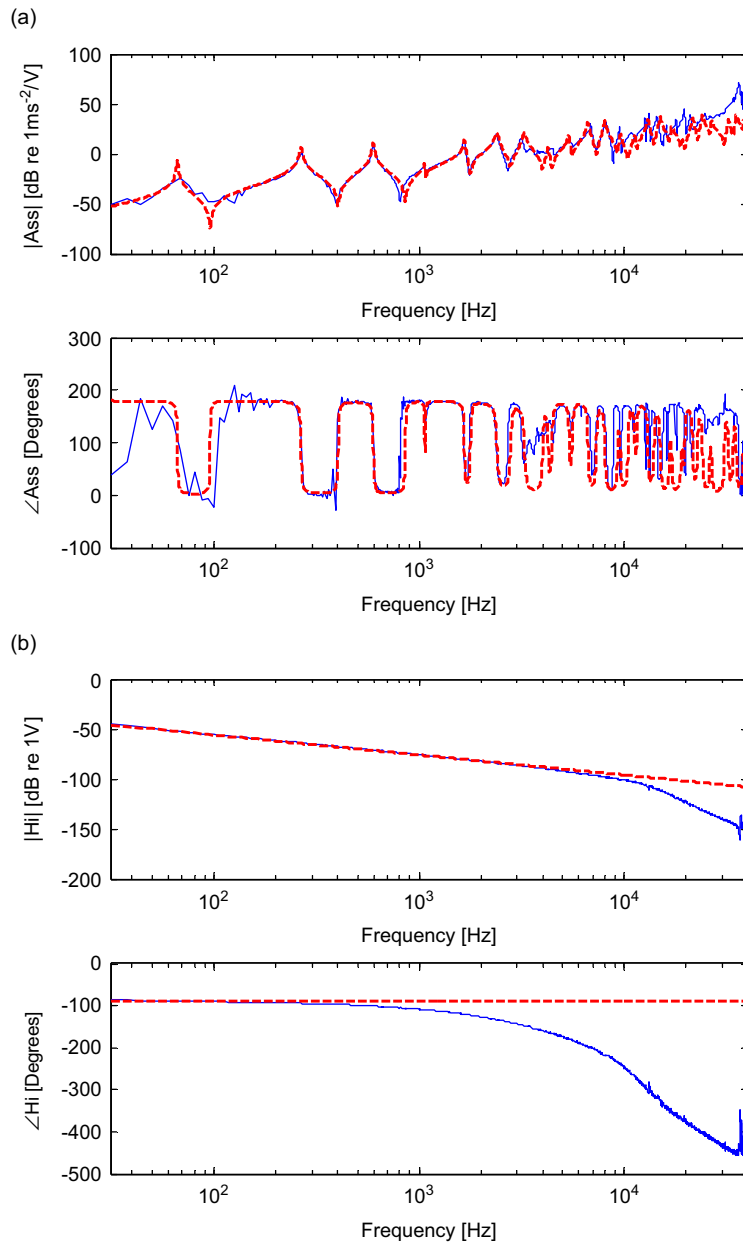
Fig. 8. Measured frequency responses of the components in the feedback loop: (a) FRF of the combination of the beam, accelerometer and piezoelectric actuator: —— measured; - - - - theoretical; (b) FRF of the integrator/power amplifier unit: —— measured; - - - - ideal.

discussed in Ref. [21], where second order filters are used to add active damping at the resonance frequencies, and the filters roll-off above their resonance frequencies. Of course, this means that a more complex controller is required. An alternative approach is to force the response of the structure to roll-off with frequency. This can be achieved by attaching a point mass to the structure at the accelerometer position, as depicted in the sketch of Fig. 13. It is to be noticed that at such high frequencies, as those being considered, the dynamic response of the accelerometer also plays an important role in determining the sensor–actuator response, as discussed by Gardonio et al. [22].

The kinetic energy of the beam with added mass may be estimated again using Eq. (5), where, in order to take into account for the presence of the point mass, the r-length vector of velocities is written as
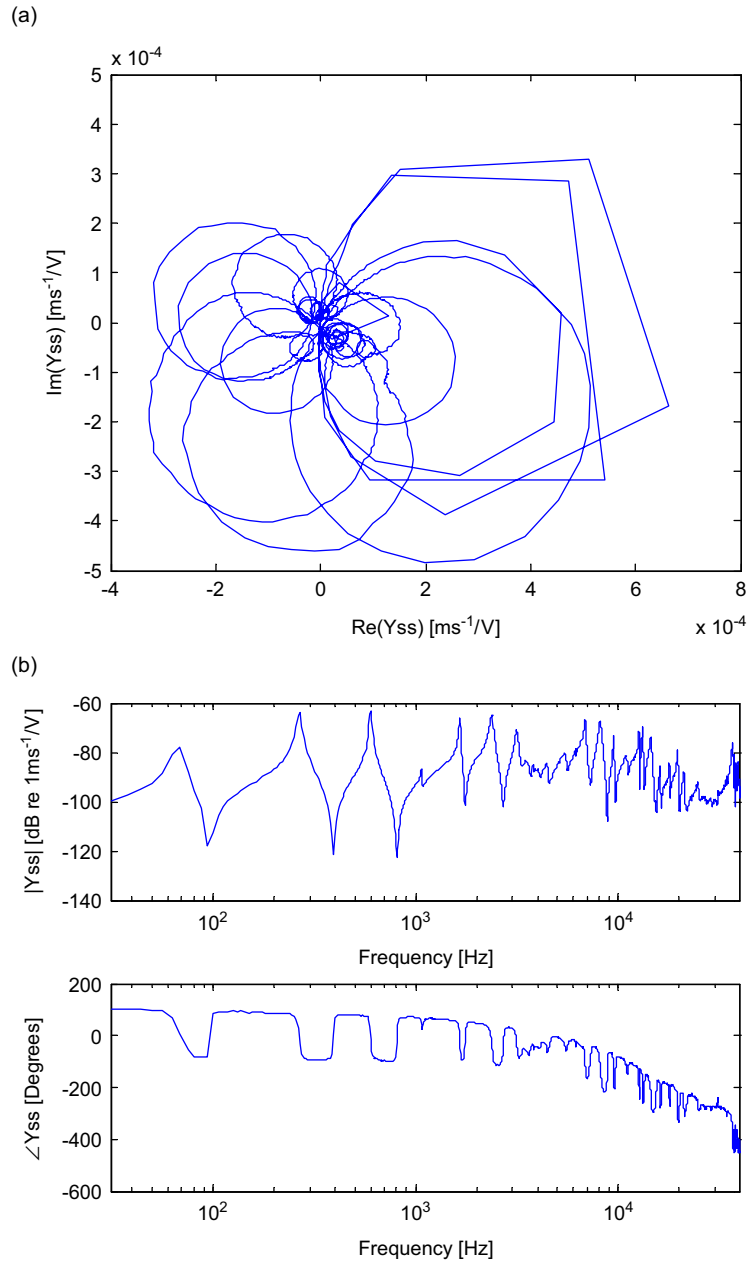
(a)

(b)

Fig. 9. Open-loop FRF (simulation based on measurements): (a) Nyquist plot, (b) Bode plot.

$\mathbf{v}^{\mathrm{T}} = \{v_1, v_2, \ldots, (\sqrt{m_a + m/r}/\sqrt{m/r})v_s, \ldots, v_r\}$ (in this case, r being such that the centre of the sth beam element coincides with the sensor location). Each velocity is now due to either the primary and secondary moment-pairs or the force F_m due to the point mass m_a, i.e. $\mathbf{v} = \mathbf{v_p} + \mathbf{v_s} + \mathbf{v_m}$. This can be written in terms of the vectors of mobilities, $\mathbf{y_p}, \mathbf{y_s}, \mathbf{y_m}$, where this latter is related to the velocities by $\mathbf{v_m} = \mathbf{y_m} F_m$, and $\mathbf{y_m} = \{Y_{m1}, Y_{m2}, \ldots, Y_{mr}\}$, with the mobility of the beam due to a point force given by

$$Y_{mr} = \frac{v(x_r)}{F_m} = j\omega \sum_{n=1}^{\infty} \frac{\phi_n(x_r)\phi_n(x_s)}{M_n(\omega_n^2(1 + j\eta) - \omega^2)}.$$
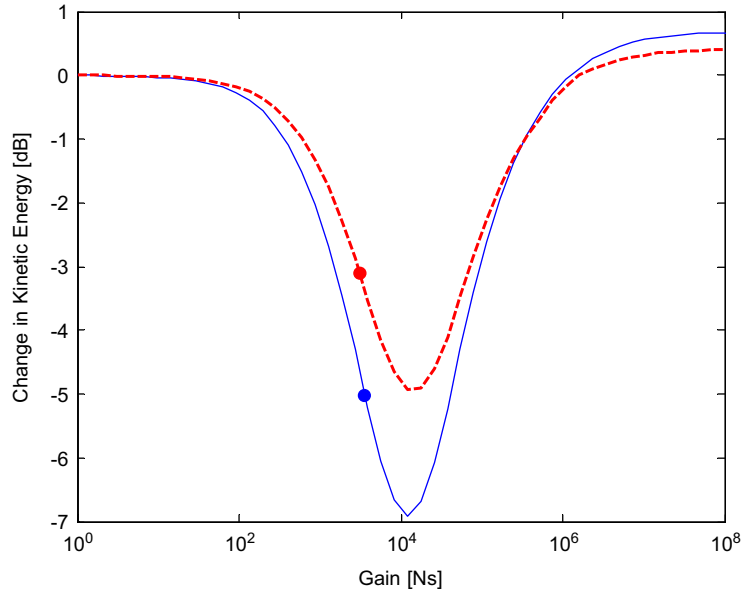
Fig. 10. Change in kinetic energy in the frequency band 0–3.2 kHz : —— theoretical simulation; ---- off-line simulation based on measured data.
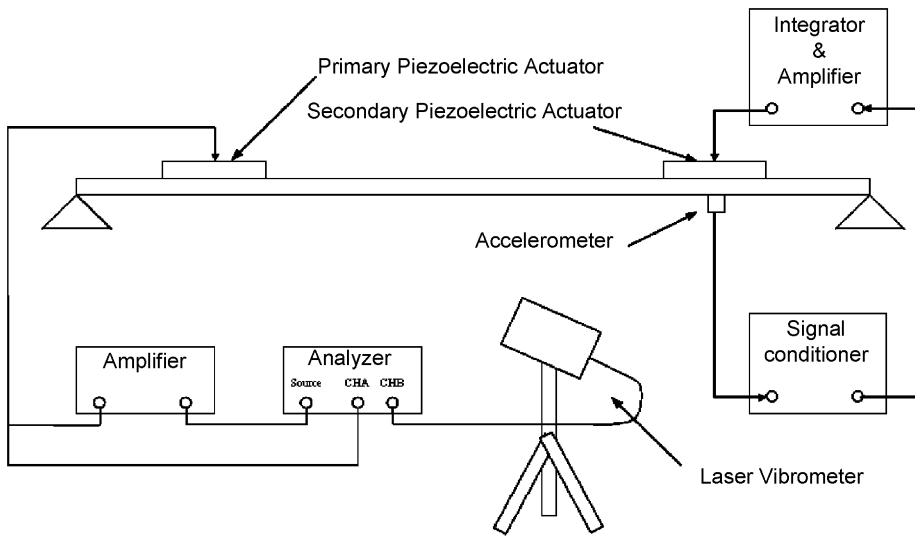

Fig. 11. Experimental set-up for the feedback control tests.

The velocity at the sensor position is now written as $v_s = Y_{ps}M_p + Y_{ss}M_s + Y_{ms}F_m$, where $F_m = -v_s/Y_m$ is the force applied to the beam by the attached point mass and $Y_m = 1/j\omega m_a$ is its mobility. It should be noted that the mobility of the point mass reduces with frequency, which has the effect of causing a roll-off in the open-loop FRF of the system.

The kinetic energy of the mass-modified system may be evaluated using Eq. (5) and the new expression for the vector of velocities given by

$$\frac{\mathbf{v}}{M_p} = \left(\mathbf{y_p} - \mathbf{y_m}\frac{Y_{ps}}{Y_m + Y_{ms}}\right) + \left(\mathbf{y_s} - \mathbf{y_m}\frac{Y_{ss}}{Y_m + Y_{ms}}\right)\frac{-gY_{ps}(Y_m/(Y_m + Y_{ms}))}{1 + gY_{ss}(Y_m/(Y_m + Y_{ms}))}. \tag{13}$$
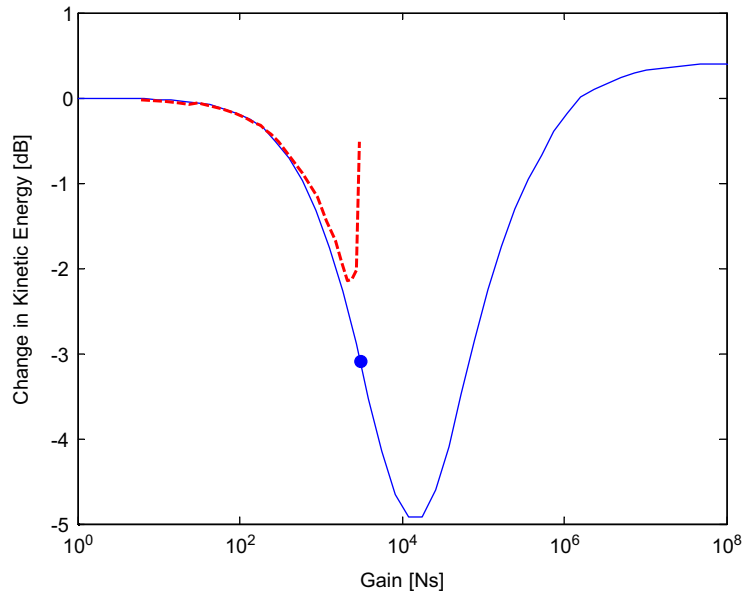
Fig. 12. Change in kinetic energy in the frequency band 0–3.2 kHz: —— simulation based on measured data; - - - - experimental results.
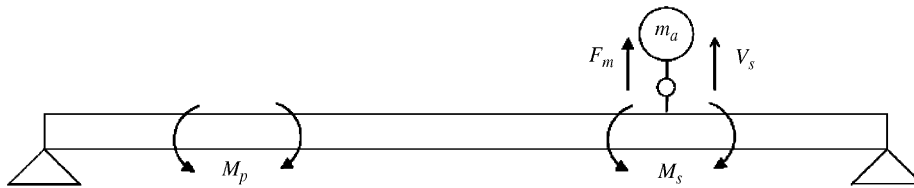

Fig. 13. Sketch of the beam with attached point mass at sensor location.

Inspection of Eq. (13) shows that the open-loop response function is modified by the term $Y_m/(Y_m + Y_{ms})$. This results in an increase of the stability margin such that a much larger gain can be applied.

The critical gain may be estimated by studying the Nyquist plot of the open-loop FRF, for different values of the attached point mass expressed as a percentage of the mass of the beam, and the corresponding kinetic energy reduction may be evaluated. This is plotted in Fig. 14 together with the ideal minimum reduction not considering stability issues. It shows that the minimum kinetic energy for the case limited by stability requirements reaches the minimum for the ideal system when m_a is greater than about 15% of the beam mass.

If, for example, a point mass of 10% of the beam mass is attached, the reduction in kinetic energy that could be achieved before the system becomes unstable is about 8 dB as shown in Fig. 15. The corresponding predicted kinetic energy as a function of frequency is shown in Fig. 16 where the maximum gain of 13627 N s has been applied.

5. Effect of damping in the beam

Throughout the paper a damping ratio of 0.01 has been assumed for the beam, and this was found to be a reasonably accurate estimate of the actual damping of the beam used in the experiments. Further simulations were conducted to determine the effect of damping on the feedforward and feedback control strategies. For feedforward control, it was found, that higher damping had no effect on the kinetic energy after control
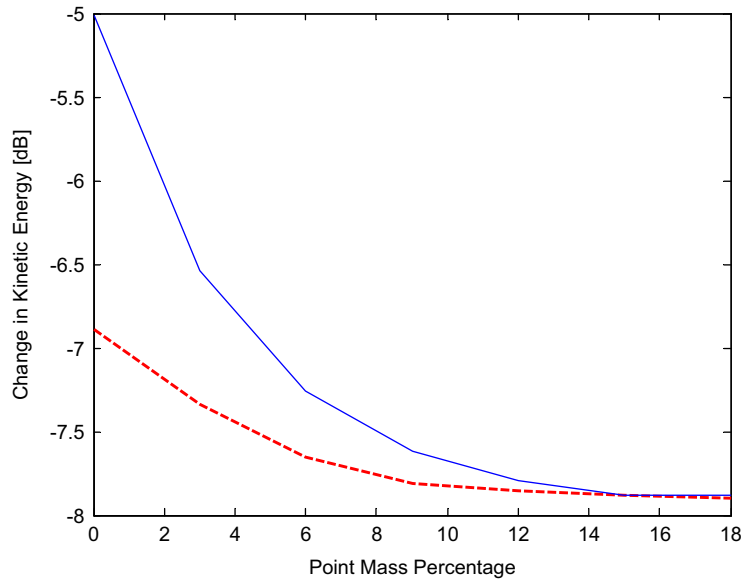
Fig. 14. Kinetic energy reduction in the frequency band 0–3.2 kHz as a function of the percentage of the point mass compared to the beam mass: —— limited by stability; - - - - ideal minimum.
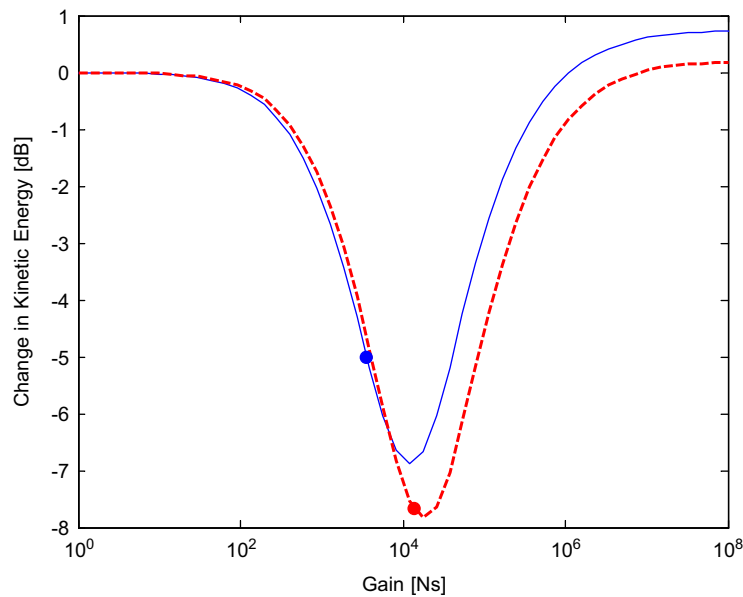

Fig. 15. Effect of adding a point mass on the reduction of the kinetic energy: —— $m_a = 0\%$; - - - - $m_a = 10\%$.

(as expected). This means that the effectiveness (the overall kinetic energy reduction in the frequency band of interest (0–3.2 kHz)), as defined at the end of Section 2 is not as good, because the kinetic energy of the beam before control is less due to the inherent damping. For feedback control, it was found that the overall kinetic energy can be reduced if damping in the beam is increased, but this is largely due to the inherent damping rather than feedback control. Thus, it can be concluded that the feedforward and feedback control strategies are most effective—compared to the uncontrolled case—when the damping in the beam is light.
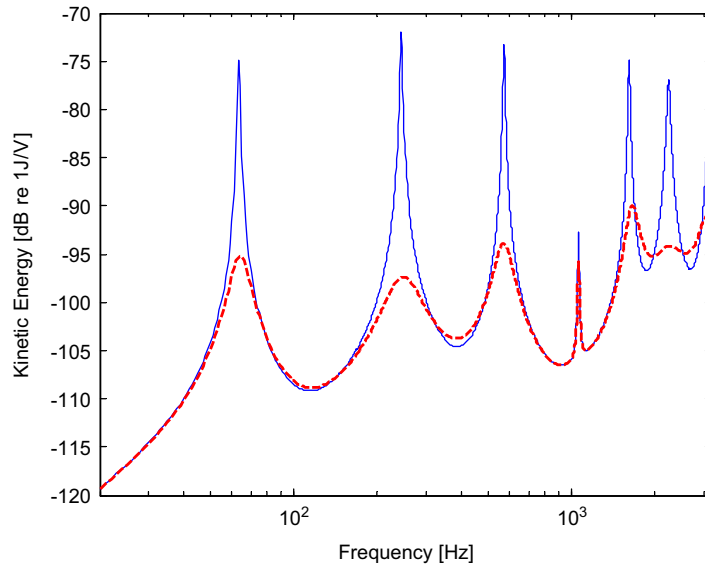
Fig. 16. Kinetic energy of the beam with velocity feedback control and a point mass of 10% of the mass of the beam applied at the accelerometer position: —— uncontrolled; - - - - $g = 13627$ N s.

6. Conclusions

This paper has described a study into DVFB control of beam vibration. The aim was to investigate the effectiveness of such a simple control system using a single accelerometer and a piezoelectric patch actuator. The accelerometer and the actuator do not form a collocated pair in the control sense so the feedback control system was only conditionally stable. The results were compared with a feedforward approach.

In the experimental work, the performance was limited by the non-ideal performance of the integrator and amplifier. However, the fundamental limitation with the piezoelectric actuator/accelerometer pair is because the structural response does not roll-off with frequency. To achieve this, and to improve the performance of the system, a point mass of 10% of the total mass of the beam was added at the accelerometer position. The resulting overall reduction of the kinetic energy in the frequency band 0–3.2 kHz was about 8 dB for velocity feedback control and about 11.5 dB for feedforward control.

References

[1] R. Alkhatib, M.F. Golnaraghi, Active structural vibration control: a review, *The Shock and Vibration Digest* 35 (5) (2003) 367–383.
[2] C.R. Fuller, S.J. Elliott, P.A. Nelson, *Active Control of Vibration*, Academic Press, New York, 1997.
[3] A. Preumont, *Vibration Control of Active Structures: An Introduction*, second ed., Kluwer Academic, Dordrecht, 2002.
[4] R.L. Clark, W.R. Saunders, G.P. Gibbs, *Adaptive Structures*, first ed., Wiley, New York, 1998.
[5] T.H. Rockwell, J.M. Lawther, Theoretical and experimental results on active vibration dampers, *Journal of the Acoustical Society of America* 36 (2) (1964) 1507–1515.
[6] B.R. Mace, Active control of flexural vibrations, *Journal of Sound and Vibration* 114 (2) (1987) 253–270.
[7] P.B. Baillargeon, S.S. Vel, Exact solution for the vibration and active damping of composite plates with piezoelectric shear actuators, *Journal of Sound and Vibration* 282 (3–5) (2005) 781–804.
[8] G. Song, P. Qiao, V. Sethi, A. Prasad, Active vibration control of a smart pultruded fiber-reinforced polymer I-beam, *Smart Materials and Structures* 13 (4) (2004) 819–827.

[9] P.B. Baillargeon, S.S. Vel, Active vibration suppression of sandwich beams using piezoelectric shear actuators: experiments and numerical simulations, *Journal of Intelligent Material Systems and Structures* 16 (6) (2005) 517–530.

[10] C.M.A. Vasquesa, J.D. Rodrigues, Active vibration control of smart piezoelectric beams: comparison of classical and optimal feedback control strategies, *Computers & Structures* 84 (22–23) (2006) 1402–1414.

[11] S.J. Elliott, P. Gardonio, T.C. Sors, M.J. Brennan, Active vibroacoustic control with multiple local feedback loops, *Journal of the Acoustic Society of America* 111 (2002) 908–915.

[12] M.J. Balas, Direct velocity feedback control of large space structures, *Journal of Guidance and Control* 2 (1979) 252–253.

[13] R.H. Cannon Jr., D.E. Rosenthal, Experiments on control of flexible structure with noncollocated sensors and actuators, *Journal of Guidance and Control* 7 (1984) 546–553.

[14] Q. Zhang, S. Shelley, R.J. Allemang, Active damping design of flexible structures based on SISO and SIMO non-collocated sensor/actuator velocity feedback, *Journal of Dynamic Systems Measurement and Control—Transactions of the ASME* 113 (1991) 159–266.

[15] E.F. Crawley, J. deLuis, Use of piezoelectric actuators as elements of intelligent structures, *AIAA Journal* 25 (1987) 1373–1385.

[16] J.S. Burdess, J.N. Fawcett, Experimental evaluation of a piezoelectric actuator for the control of vibration in a cantilevered beam, *Proceedings of the Institution of Mechanical Engineers* 206 (1992) 99–106.

[17] W. Variyart, M.J. Brennan, S.J. Elliot, Active damping for a beam using feedback control, *Proceedings of Active 2002*, Institute of Sound and Vibration Research, Southampton, 15–17 July 2002.

[18] C. Hong, S.J. Elliott, Active control of resiliently-mounted beams with a moment pair actuator, *Smart Materials and Structures* 14 (2005) 727–738.

[19] P. Gardonio, S.J. Elliott, Modal response of a beam with a sensor–actuator pair for the implementation of velocity feedback control, *Journal of Sound and Vibration* 284 (2005) 1–22.

[20] M.J. Brennan, S.J. Elliott, R.J. Pinnington, The dynamic coupling between piezoceramic actuators and a beam, *Journal of the Acoustical Society of America* 102 (4) (1997) 1931–1942.

[21] M.I. Friswell, D.J. Inman, The relationship between positive position feedback and output feedback controllers, *Smart Materials and Structures* 8 (3) (1999) 285–291.

[22] P. Gardonio, E. Bianchi, S.J. Elliott, Smart panel with multiple decentralised units for the control of sound transmission, part II: design of the decentralised control units, *Journal of Sound and Vibration* 274 (2004) 193–213.